I-A 2 FAILURE STRAIN OF THIN-WALLED STEEL PIPE STUB-COLUMNS UNDER COMBINED COMPRESSION AND BENDING

Nagoya University Student Member ○ Shengbin Gao
Nagoya University Member Hanbin Ge
Nagoya University Fellow Member Tsutomu Usami

1. Introduction

Use of steel in bridge piers is now becoming more and more popular. Steel bridge piers are normally constructed as cantilever columns or planar rigid frames. The common cross-sectional shapes are thin-walled box sections or pipe sections. The load-deformation behavior of such members can be computed using a large-displacement FEM analysis and its ultimate strength and deformation are obtained based on a faliure criterion for which failure strains of sections are used. In the case of steel box sections, an empirical formula for the failure strain has been proposed by authors [1]. For pipe sections, however, there is no research work available on the failure strain.

This paper presents an elasto-plastic finite displacement analysis of thin-walled steel pipe stub-columns under pure compression or combined compression and bending to develop some simple formulas for engineering design. A type of four-node doubly curved shell element (S4R5) included in the ABAQUS is employed. Both initial imperfection and residual stress are considered. An elasto-plastic strain hardening model [1] is adopted to considered material nonlinear behavior. The effects of various parameters such as the initial deflection, radius-thickness ratio, and length-radius ratio on the ultimate strength and deformation of cylinders are investigated. As a result, a set of formulas for the ultimate strength and failure strain of thin-walled cylinders in compression are proposed.

2. Analytical Method

Because of symmetry about the mid-surface in longitudinal direction, a half or a quarter of the upper half of the cylinder is analyzed respectively, corresponding to whether the residual stress is considered or not. The cylinder is divided into fifteen equal parts for the former case and six equal parts for the latter case along the circumferential direction, and eight equal parts along the longitudinal direction for both cases, as shown in Fig. 1. A type of four-node doubly curved shell element (S4R5) included in the ABAQUS software is adopted to analyze the cylinder. Finite element meshes of the cylinder are also shown in Fig. 1. Sinusoidal initial geometrical imperfection is considered both in the longitudinal and circumferential directions. The following initial deflection equation is assumed.

$$\omega = \omega_{max} \sin(\frac{m\pi x}{L}) \sin(\frac{ny}{R}) \quad (1)$$

where ω is the outward displacement at local coordinate (x, y), ω_{max} is the magnitude of maximum initial deflection, y is the curvilinear coordinate along the circumferential direction, m and n are the number of sine-waves along the longitudinal and circumferential direction, and equal to 1 and 2, respectively. An idealized form of residual stress distribution due to welding is used in this study. The validity of the present model is examined by comparing the computed results with analytical results by Gunawardena and Usami [2] and test results by Usami et al. [3].

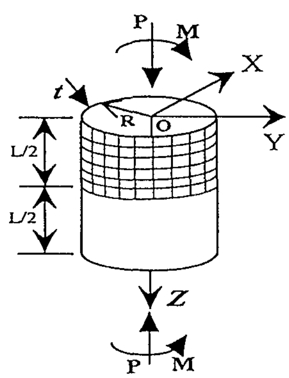

Fig. 1 Analytical Model

3. Numerical Results

The radius-thickness ratio parameter, R_t, is defined by

$$R_t = \frac{\sigma_y}{\sigma_E} = 1.65\frac{\sigma_y}{E} \cdot \frac{R}{t} \quad (2)$$

Here, σ_y is yield stress, σ_E is the elastic buckling stress, E is Young's modulus, R and t denote the radius and thickness of cylinder, respectively.

The cylinders are made of SS400 steel with the properties of σ_y=235.2 Mpa, E=206 GPa, ν=0.3, $\varepsilon_{st}=10\varepsilon_y$, and $E_{st}=E/40$. The thickness of the cylinders is assumed as 20 mm, and the scope of L/R is taken from 0.1 to 0.4 for the following four R_t values: 0.0625, 0.1250, 0.1875 and 0.25, respectively. The magnitude of maximum initial imperfection ω_{max} is taken as $0.0025L$ which represents the average value of maximum measurements [3], and the maximum compressive residual stress σ_{rc} is $0.3\sigma_y$.

Average stress-average strain curves of axially loaded cylinders are computed and the obtained ultimate strengths σ_u/σ_y are shown in Fig. 2 against the ratio L/R for different values of R_t. It can be observed that for the same R_t there is always an critical L/R value which gives the lowest ultimate strength, while all others predict a higher peak load. These critical lengths of cylinders are plotted against R_t in Fig. 3. An equation to fit the computed results is

$$\frac{L}{R} = \frac{1.17}{R_t^{0.08}} - 1.16 \qquad (3)$$

This equation will be used to determine the cylinder length in the analysis presented later.

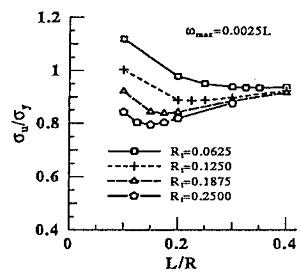

Fig. 2 Effect of R_t on σ_u/σ_y

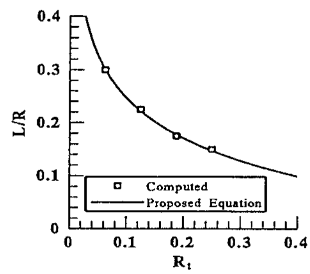

Fig. 3 L/R — R_t Curve

To study the effect of R_t on the ultimate strength and postbuckling behavior, nine cylinders with different values of R_t ranging from 0.03 to 0.5 are analyzed. The computed ultimate strengths are plotted against R_t and shown in Fig. 4. In this figure, a solid line denotes an empirical equation proposed by Usami [3]. This equation represents an average strength curve of test results. It is obvious that all the computed results are a little lower than the empirical equation. The following equation is found to give a satisfactory fit to the computed ultimate strength

$$\frac{\sigma_u}{\sigma_y} = 1 - 0.43\sqrt{R_t - 0.03} \qquad (R_t \geq 0.03) \qquad (4)$$

When R_t=0.03, we have σ_u/σ_y=1.0, and it implies that no local buckling would occur at this value.

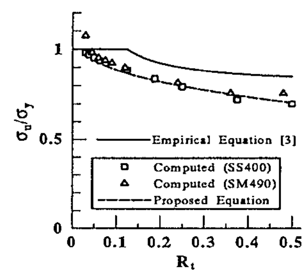

Fig. 4 Computed Ultimate Strengths

The curve of failure strains versus R_t is plotted in Fig. 5. The failure strain taken here is defined as a point with 95% of the ultimate strength after the peak. As indicated in Fig. 5, the failure strain is very sensitive to R_t for cylinders of $R_t \leq 0.1$. The equation of nondimensional failure strain $\varepsilon_{u,s}/\varepsilon_y$ versus R_t is fitted as follows.

$$\frac{\varepsilon_{u,s}}{\varepsilon_y} = \frac{0.445}{(R_t - 0.03)^{0.6}} + 1.0 \qquad (0.03 < R_t \leq 0.5) \qquad (5)$$

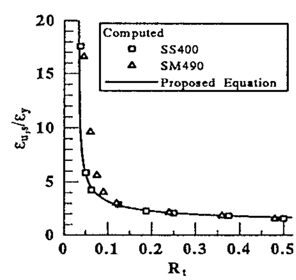

Fig. 5 Computed Failure Strains

To investigate the validity of the proposed equations for different materials, cylinders of SM490 steel with the same initial imperfection as in the case of the SS400 material are analyzed. The input data of the SM490 material properties used are σ_y=313.6 MPa, E=206 GPa, ν=0.3, $\varepsilon_{st}=7\varepsilon_y$, and $E_{st}=E/30$. The computed results are also plotted in Figs. 4 and 5, respectively. For the same small R_t ratios, the cylinder of SM490 predicts larger failure strain than that of SS400 because of the different effect of yield plateau and strain hardening. From Figs. 4 and 5, it can be concluded that Eqs. 4 and 5 obtained from the SS400 material are also applicable for cylinders made of the SM490 material and will give a safe-side predictions.

4. Conclusions

Analyses of cylinders under combined compression and bending are under the way and their results are to be reported at presentation.

5. References

[1] Usami, T. et al., Proc. of JSCE, No.525/I-33, pp.69-82, 1995. [2] Gunawardena, S. R. and Usami, T., Struct. Eng. / Earthquake Eng., JSCE, Vol.7, No.1 pp.55s-65s, 1990. [3] Usami, T. et al., Proc. of JSCE, No.416/I-13, pp.256-264, 1990.